Measurements of ion energy distributions by Doppler shift spectroscopy in an inertial-electrostatic confinement device

J. Khachan[a] and S. Collis
Department of Plasma Physics, School of Physics, University of Sydney, 2006 Australia

(Received 30 October 2000; accepted 20 December 2000)

Doppler shift spectroscopy was carried out on the discharge in a spherically symmetric inertial-electrostatic confinement system. This enabled the ion energy distributions, types, and densities of ionic species to be determined. A weakly ionized hydrogen radio-frequency discharge was used as the ion source for two spherical and concentric electrostatic grids. The inner and outer grids were the cathode and anode, respectively. It was found that the ion energy distribution consisted of a non-Maxwellian directional component, as well as a spatially isotropic Maxwellian distribution. The directional component consisted of three broadened energy peaks belonging to H_3^+ (20%), H_2^+ (60%), and H^+ (20%). These ions had energies approximately 20% of the cathode potential. The temperature (in electronvolts) of the Maxwellian distribution was approximately 15% of the cathode potential. © *2001 American Institute of Physics.* [DOI: 10.1063/1.1349875]

I. INTRODUCTION

Confinement of light nuclei in a deep electrostatic potential well for nuclear fusion[1–4] is a concept that dates as far back as magnetic fusion but has not received the same degree of attention. There have been several experimental configurations[5–7] for producing a spherically or cylindrically symmetric electrostatic potential well.

Typically, ions are injected radially into the well and converge to the center resulting in a core of higher ion density. Provided the well is sufficiently deep, the ions will acquire sufficient energy to undergo nuclear fusion reactions. Many ions will make multiple passes through the center before a collision occurs. This idealized picture of a particle being trapped by an electrostatic well is an important feature of such devices, which have consequently been called inertial-electrostatic confinement (IEC) devices. This arrangement is also known as spherically convergent ion focus. It is expected that this device has the potential to be used as a simple, portable, turn-key neutron source, from deuterium-deuterium fusion reactions.[8]

The ion energy distribution established during steady state operation is one of the main factors that determines the number of fusion reactions. Ideally, the distribution should be monoenergetic with one specie. However, it has been suggested[9] that collisions will relax the energy distribution to a Maxwellian very quickly leading to energetic ions in the tail of the distribution being lost from the well.

In this paper, we report on measurements of the ion energy distributions of the different ionic species that are created in such discharges. This was carried out by measuring the Doppler shift of the hydrogen H_α line, which is emitted from the $n=3$ to $n=2$ levels of excited hydrogen atoms that result from charge-exchange reactions with the accelerated ions. The resulting spectrum was used to determine the relative densities of the different ionic species that are created.

II. EXPERIMENTAL APPARATUS

Figure 1 shows a schematic diagram of the IEC system used in this study. It consists of two concentric and spherically symmetric grids. The outer and inner grids are the anode and cathode, respectively. The inner grid was made from three orthogonal rings with a common center. Each ring had a diameter of 30 mm and made from 1.5 mm diam stainless steel wire. This arrangement of rings produced an open spherical grid that consisted of eight triangular faces. The outer grid had a diameter of 120 mm and was made from fine-wire brass mesh with a wire spacing of 2 mm.

The concentric grids assembly was immersed in a hydrogen plasma generated by a radio-frequency discharge at 13.56 MHz at a pressure that ranged from 1 to 20 mTorr. The outer grid was held at the same potential as the chamber that contained the plasma. The plasma on the outside of the spherical mesh was kept at very low densities so that the grid spacing was of the order of a Debye length, which greatly reduced the density of the plasma that penetrated through the mesh. Ions that drifted through to the inside of the outer grid (anode) were accelerated towards the inner grid (cathode). The current collected by the cathode was about 1 mA. The anode also acted as a radio-frequency radiation shield for the ions being accelerated within it. The high transparency of the cathode (85%) resulted in many ions continuing their trajectory to the center.

A striking feature of this type of discharge is the formation of straight channels of optical emission through the center of the triangular faces of the cathode. These eight channels intersect in the center where the intensity of the discharge is greatest.

The channels are due to excited atomic hydrogen, which will be discussed in the next section. The hydrogen H_α line (656.3 nm) was detected with an intensified charge-coupled

[a]Electronic mail: khachan@physics.usyd.edu.au

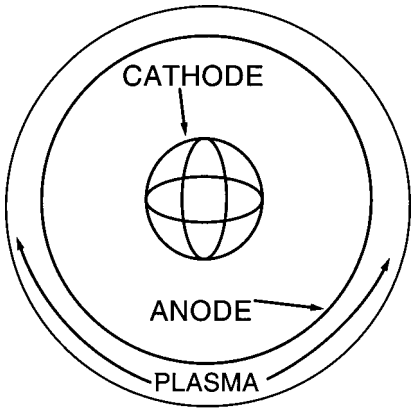

FIG. 1. Schematic diagram of the IEC system.

device (Princeton Instruments ICCD 576G/RB-E) mounted on a 0.5 m focal length monochromator (Spex 500M). The resolution of the set-up was 0.04 nm.

A second phase to the experiment was the study of a single channel and the dependence of the observed spectrum on the angular position of the channel with respect to the line-of-sight of the monochromator entrance slit. To eliminate any contribution from the other channels, the cathode was replaced with two parallel, 20 mm diam rings that were separated by 20 mm with their centers on the same axis. The rings had the same potential placed on them, which produced a spatial potential profile along the axis similar to the potential along a line through the centers of two opposing triangles on the three-ring grid. This resulted in a single light-channel through the centers of the rings.

III. EXPERIMENTAL RESULTS AND ANALYSIS

We will omit the negative sign from all references to the potentials placed on the inner grid since no other polarity was used. Figure 2 shows the spectrum of the H_α line from the core of the discharge when the three-ring cathode was biased at 12 kV at pressures of 5 and 20 mTorr. None of the eight channels were directed towards the spectrometer. The line shape is composed of two components: a sharp central peak with its base broadened and ''wings'' on either side of the central line. The sharp central line is the characteristic H_α of hydrogen and results largely from electron impact with atomic and molecular hydrogen. The broadened base is also due to electronic processes, which has been treated elsewhere[10] and is not the main concern of this paper since it does not directly offer any information about ion energies.

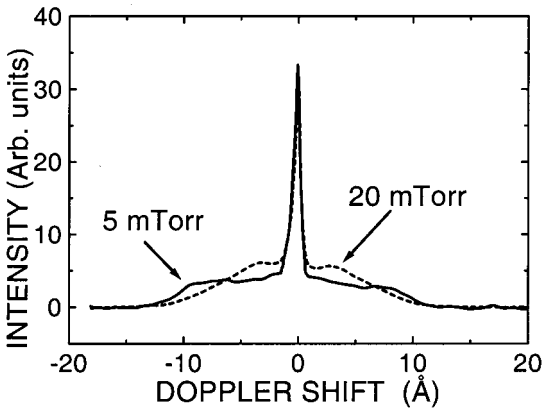

FIG. 2. The spectrum of the H_α line from the center of the three-ring cathode, biased at 12 kV at pressures of 5 and 20 mTorr.

More striking, is the large broadening (''wings'') on both sides of the central line. These result from the Doppler shift of the H_α line. Consequently, it is a simple matter to workout the energy of these hydrogen neutrals. The shift in wavelength, $\Delta\lambda$, is given by

$$\Delta\lambda \approx \frac{v\lambda_0}{c}\cos\theta, \tag{1}$$

where λ_0 is the wavelength of the unshifted H_α line, v is the speed of an excited atomic hydrogen, c is the speed of light, and θ is the angle between the observation direction and the radiator. Therefore, the kinetic energy, K, of an excited neutral is given by

$$K = \frac{m_H c^2 (\Delta\lambda)^2}{2\lambda_0^2 \cos^2\theta}, \tag{2}$$

where m_H is the mass of atomic hydrogen. The highest shift is between 1 and 1.5 nm, which corresponds to an energy between 1 and 2 keV. This energy is clearly too large to arise from electron impact processes and can only result from the following charge-exchange reactions:

$$\begin{aligned}
&H^+ + H \rightarrow H^* + H^+,\\
&H_2^+ + H \rightarrow H^* + H + H^+,\\
&H_3^+ + H \rightarrow H^* + H_2 + H^+,\\
&H^+ + H_2 \rightarrow H^* + H_2^+,\\
&H_2^+ + H_2 \rightarrow H^* + H + H_2^+,\\
&H_3^+ + H_2 \rightarrow H^* + H_2 + H_2^+.
\end{aligned} \tag{3}$$

Ions (H^+,H_2^+,H_3^+) from the plasma, are accelerated by the electric field between the anode and cathode. A fraction of them are involved in charge-exchange reactions with atomic hydrogen (H) and the background gas (H_2). This results in energetic and excited neutrals, H*, that emit the Doppler shifted part of the spectrum. It has been shown[11] that the fast neutrals have trajectories that are in the same direction as the incident ions. Any beam spreading is between one and three degrees, depending on the energy of the incident beam. Moreover, the total energy of the resulting fragments from the reactions is approximately equal to the energy of the incident ion. Any energy lost to electronic or vibrational excitation are only a few tens of eV and are negligible compared to the keV range of energies considered here. Note that the 5 mTorr spectrum in Fig. 2 is broader than the 20 mTorr spectrum. This implies that the average ion energy is higher at 5 mTorr. However, the interpretation of such spectra will become clear during the course of this paper.

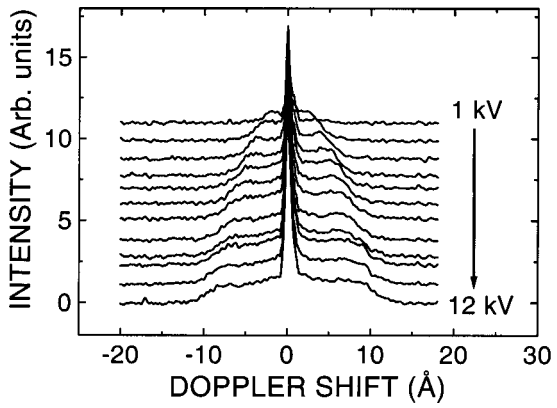

FIG. 3. Increasing Doppler shift spectrum with increasing cathode voltage.

Figure 3 shows the increasing Doppler shift with increasing cathode voltage in 1 kV increments. The plots have been artificially shifted vertically with respect to each other for clarity. There is a linear dependence of the shift in wavelength at the turning point (''knee''), near the ends of the Doppler shift, and the square root of the applied voltage, as shown in Fig. 4. This implies that the excited neutrals result from ions that are being accelerated by the applied potential. Consequently, these excited neutrals can only result from charge-exchange collisions with the accelerated ions. The interpretation of such spectra can be problematic because it is uncertain whether the spread in the observed shift is due to a combination of the angular dependence of the Doppler shift from the different channels, and scattering and thermalization of the incident ions. We will show this combination to be the case.

It can be shown that spherically convergent, monoenergetic, excited neutrals will give a Doppler shifted spectrum that is flat up to a maximum shift, where the intensity sharply falls to zero. At first sight, this would appear to be the spectrum obtained in Fig. 3. However, the same spectrum was obtained near the edge of the cathode away from the core. This is surprising since it implies the spectrum is a characteristic of other parts of a channel rather than specific to the core. On closer examination, the spectrum is not truly flat but has some structure. It was not possible to collect light from a single channel without a substantial contribution from another channel. To simplify matters, a single channel was examined by using the two-ring grid. The axis of the channel was rotated through several angles with respect to the line-of-sight of the monochromator entrance slit. The spectrum was obtain between the two rings for all angles except 0°, where the full length of the channel was aligned with the line-of-sight. The results are shown in Fig. 5 for a voltage of 9.3 kV at a pressure of 5 mTorr. Clearly there is a directional beam of almost monoenergetic ions as shown by the peak that arises between 0° and 20°, which we shall call the directional component. Superimposed on this peak is an isotropic scattering of ions as shown by the same continuously shifted background for all angles. We will analyze these two components separately.

A. Directional component

The spectrum was acquired again for a light-channel axis of 0° and voltages between 1 and 10 kV at 5 mTorr. Greater vertical resolution and spectrum accumulation time were used in order to obtain a detailed profile of the line shape. A typical result is shown in Fig. 6 for 4 kV at a pressure of 5 mTorr. This shows the superposition of three peaks. We have deconvolved this three-peak spectrum into three Gaussians, also shown in Fig. 6, in order to obtain the Doppler shift of each peak.

The positions of the three peaks shifted with varying voltage. The most likely sources of this part of the spectrum are the three charge-exchange reactions of the incident H^+, H_2^+, and H_3^+ with the background hydrogen gas, H_2, given in Eq. (3). This can be verified by plotting the energy of the incident ion vs the applied potential. The energy of the incident ion can be obtained from the energy of the resulting excited neutral. For example, the energy of H_3^+ is three times the energy of the resulting H* because the energy of each fragment after charge exchange is partitioned in proportion to the mass of the particle. Similarly, the energy of H_2^+ is twice the energy of the resulting H*.

Figure 7 shows a plot of the energy of the three types of

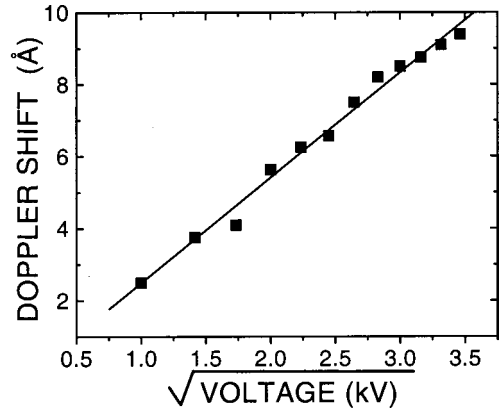

FIG. 4. A linear relationship between the ''knee'' of the Doppler shift and the square root of the applied voltage.

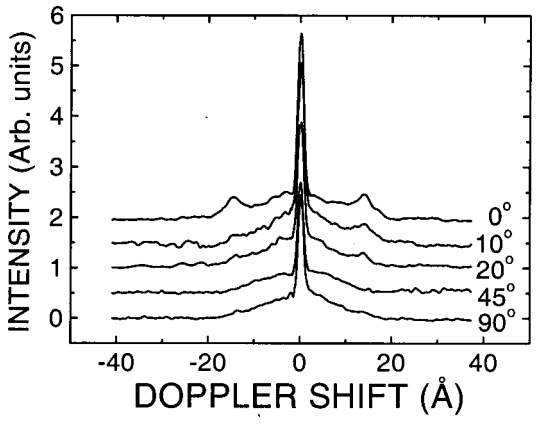

FIG. 5. Doppler shift spectrum from the center of a single channel rotated through several angles, at 9.3 kV and a pressure of 5 mTorr.

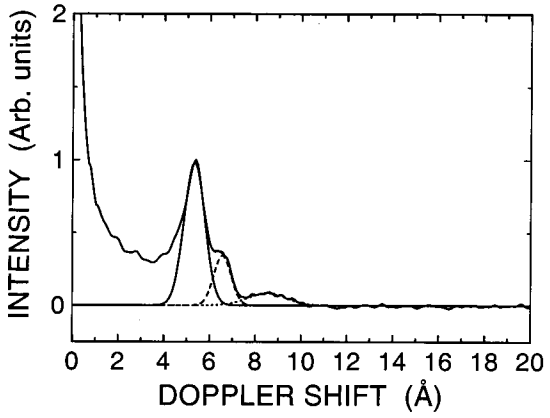

FIG. 6. Doppler shift spectrum of a single channel at 0°, at an applied voltage of 4 kV and 5 mTorr, showing three directional, and almost monoenergetic peaks.

incident ions as a function of the applied potential. Within experimental error, the energies of the three ions are nearly the same. This is to be expected since they were all accelerated by the same potential difference. As a result, this strongly supports the assumption that the three peaks in the Doppler shifted spectrum result from charge-exchange of these three ions with the background gas. The minor differences in energy may be due to the different mobilities[12] of the three different ions in hydrogen gas. Interestingly, the energies of the incident ions are approximately 20% of the applied potential. Previous models of these types of discharges assumed a monoenergetic single specie with an energy determined by the applied electric field. Clearly, collisions play a substantial role in moderating the energy of these ions.

It is also possible to determine the relative densities of the three ionic species. The total intensity, $I_n(H_x^+)$, from the H_α line due to charge-exchange between H_x^+ (where $x=1$, 2, and 3) and the background gas is given by

$$I_n(H_x^+) = h\nu A_{3\to 2} n_H(H_x^+), \tag{4}$$

where h is Planck's constant, ν is the frequency of the emitted photons, $A_{3\to 2}$ is the transition probability between the

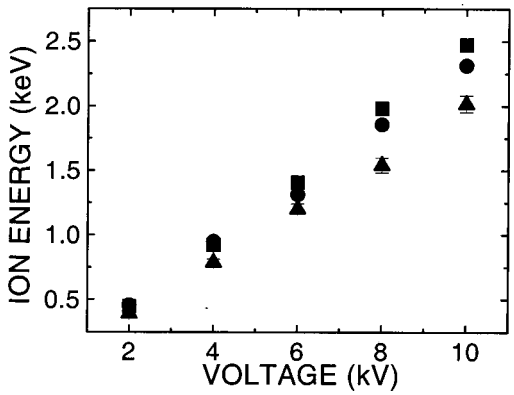

FIG. 7. Plot of the energy of the incident H_3^+(□), H_2^+(○), and H^+(△) vs applied voltage.

$n=3$ and $n=2$ energy levels of atomic hydrogen, and $n_H(H_x^+)$ is the number density of the atomic hydrogen in the $n=3$ state that results from a charge-exchange reaction between H_x^+ and the background gas. We can obtain $n_H(H_x^+)$ by considering its rate of change, $dn_H(H_x^+)/dt$, given by

$$\frac{dn_H(H_x^+)}{dt} = n_{H_x^+} n_{H_2} k_{H_x^+} - \sum_{i=1}^{2} A_{3\to i} n_H(H_x^+) - k_q n_{H_2} n_H(H_x^+), \tag{5}$$

where $n_{H_x^+}$ is the number density of incident H_x^+, n_{H_2} is the number density of the H_2 background gas, $k_{H_x^+}$ is the charge-exchange rate coefficient resulting in excited atomic hydrogen, $A_{3\to i}$ is the transition probability between the $n=3$ and $n=i$ energy levels of excited atomic hydrogen (where $i=1$, 2), and k_q is the quenching rate coefficient. We will only consider quenching due to the background gas, H_2, since its density is much greater than any other species present.[13]

Equation (5) balances the rate of production and loss of atomic hydrogen in the $n=3$ energy level. The first term on the right-hand side is the rate at which excited atomic hydrogen is created from charge-exchange collisions. The second term is the rate at which there is a loss of atomic hydrogen from the $n=3$ level due to spontaneous emission. The third term represents the loss of atomic hydrogen from the $n=3$ state due to radiationless transitions from collisions with H_2 (quenching).

For a continuous discharge, we can apply the steady state condition $dn_H(H_x^+)/dt=0$, which simplifies Eq. (5) to

$$n_{H_x^+} = \frac{(\Sigma_{i=1}^{2} A_{3\to i} + k_q n_{H_2}) n_H(H_x^+)}{n_{H_2} k_{H_x^+}}. \tag{6}$$

Assuming the quenching rate coefficient is the same for all three energy peaks and using Eq. (4), we can obtain the relative number densities of H_3^+ and H_2^+ with respect to the density of H^+. This is given by

$$\frac{n_{H_x^+}}{n_{H^+}} = \frac{k_{H^+} I_n(H_x^+)}{k_{H_x^+} I_n(H^+)}. \tag{7}$$

The intensities $I_n(H_x^+)$ were obtained from the area under the Gaussian fits of the directional peaks. The charge-exchange rate coefficients, $k_{H_x^+}$, are given by

$$k_{H_x^+} = \int \sigma_{H_x^+} v f(v) dv, \tag{8}$$

where $\sigma_{H_x^+}$ is the total charge-exchange cross-section for populating the $n=3$ energy level, v is the velocity of the incident ion, and $f(v)$ is the velocity distribution function. Since the directional peaks in the spectrum are far from Maxwellian and much closer to being monoenergetic, we will assume that the charge-exchange cross-section is constant, so that the rate coefficient now simplifies to

$$k_{H_x^+} = \sigma_{H_x^+} \bar{v}_{H_x^+}, \tag{9}$$

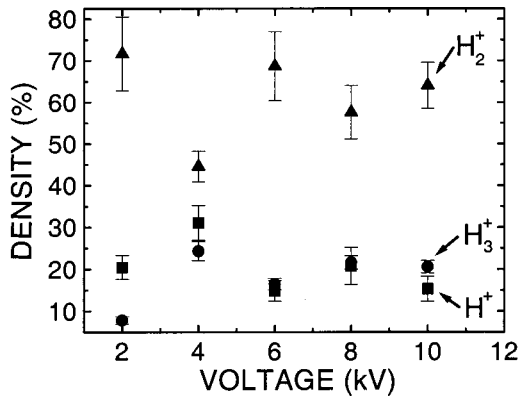

FIG. 8. The percentage of the number density H_3^+(○), H_2^+(△), and H^+(□) in a single channel vs applied voltage.

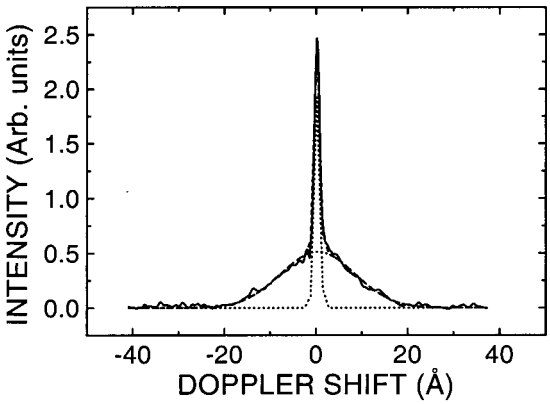

FIG. 9. A Gaussian fit to the spectrum from a 90° single channel at an applied voltage of 9.3 kV and a pressure of 5 mTorr.

where $\overline{v}_{H_x^+}$ is the average velocity of the H_x^+ ions. The density ratio now becomes

$$\frac{n_{H_x^+}}{n_{H^+}} = \frac{\sigma_{H^+}\Delta\lambda_{H^+} I_n(H_x^+)}{\sigma_{H_x^+}\Delta\lambda_{H_x^+} I_n(H^+)}, \tag{10}$$

where $\Delta\lambda_{H_x^+}$ is the Doppler shift of the peak associated with the H_x^+ incident ion. The accuracy of relative density calculations depends greatly on the accuracy of the charge-exchange cross sections for atomic hydrogen excitation, which we obtained from Phelps.[12] The calculated data also relies to a lesser extent on the accuracy of the fitting procedure for the three peaks.

Figure 8 shows the percentage of ionic species in a light-channel. These results suggest that the channel is composed of $\sim 20\% H^+$, $\sim 60\% H_2^+$, and $\sim 20\% H_3^+$. Since hydrogen is chemically equivalent to deuterium (D), then we can also assume that a similar discharge would produce similar densities of D^+, D_2^+ and D_3^+.

Clearly, for greater fusion rates the D^+ density would have to be increased. Although D_2^+ and D_3^+ will also contribute to fusion reactions, the energy per nucleon is $\frac{1}{2}$ and $\frac{1}{3}$ of the energy of D^+, respectively. This leads to reduced fusion rates since the cross sections are smaller at lower energies.

The fractions of the different ionic species shown here depend on their densities in the RF-plasma. Undoubtedly other IEC discharges will have different fractions of ionic species that are device dependent. However, it is likely in all such low power devices that the densities of the molecular hydrogen ions or molecular deuterium ions will form a substantial part of the IEC discharge, including those that use ion guns.[6]

B. Isotropic component

We will now examine ion energies that give rise to the continuous Doppler shifted spectrum. This spectrum is isotropic and mostly likely due to elastic and inelastic scattering from the background gas, as well as Coulomb scattering from counter streaming ions in the same channel. As in the directional peaks, there will be energy loss due to charge-exchange processes as well as momentum transfer to the background gas. It is shown in Fig. 9 that the 90° spectrum from Fig. 5 fits a Gaussian spectrum very well. Consequently, the ion velocity distribution that produces this spectrum must be a Maxwellian. This type of spectrum was obtained for voltages up to 16 kV and found to always have a Gaussian shape. The temperature associated with this broadening was found to always be at 15% of the applied bias at 5 mTorr. For example, Fig. 9 was obtained at a bias of 9.3 kV and found to have a temperature of 1.4 keV. This temperature, as well as the energy of the directional ions, will undoubtedly change with pressure and volume of the electrostatic system. The effect of these parameters on energy distributions as well as their effect on fusion production rates will be left for further research.

IV. CONCLUSIONS

Doppler shift spectroscopy was carried out on optical emission from an IEC device. It was found that a large component of the spectrum resulted from charge-exchange processes by energetic ions with the background gas. Moreover, the spectrum showed there were directional ion beams of H^+ ($\sim 20\%$), H_2^+ ($\sim 60\%$), and H_3^+ ($\sim 20\%$), which were almost monoenergetic. The energies of these ions (in electron-volts) were $\sim 20\%$ of the applied voltage to the cathode. Superimposed on these ionic beams was a large, isotropic, Maxwellian velocity distribution of ions with a temperature $\sim 15\%$ of the applied voltage to the cathode.

It was found that the energies of ions and the resulting neutrals (in the units of mTorr pressure range) at the core are the same as those in the channels away from the core. Since the density of ions in the channels are a few orders of magnitude less than the density of the background gas, it is not surprising that some research[14] has shown that most fusion reactions occur with the background gas outside of the core. A theoretical treatment to estimate the full potential of these devices as neutron sources must include both the different types of species and both the monoenergetic and Maxwellian components. Moreover, the energies of these components

would have to be moderated by the background gas through processes such as charge-exchange and momentum transfer. This will be left for future work.

[1]W. C. Elmore, J. L. Tuck, and K. M. Watson, Phys. Fluids **2**, 239 (1959).
[2]O. A. Lavrent'ev, Ukr. Fiz. Zh. **8**, 440 (1963).
[3]P. T. Farnsworth, U.S. Patent No. 3 258 402, 1966.
[4]P. T. Farnsworth, U.S. Patent No. 3 386 883, 1968.
[5]R. L. Hirsch, J. Appl. Phys. **38**, 4522 (1967).
[6]R. L. Hirsch, Phys. Fluids **11**, 2486 (1968).
[7]G. H. Miley, J. Nadler, T. Hochberg, Y. Gu, O. Barnouin, and J. Lovberg, Fusion Technol. **19**, 840 (1991).
[8]G. H. Miley, Nucl. Instrum. Methods Phys. Res. A **422**, 16 (1999).
[9]T. H. Rider, Phys. Plasmas **2**, 1853 (1995).
[10]C. Barbeau and J. Jolly, J. Phys. D **23**, 1168 (1990).
[11]G. W. McClure, Phys. Rev. **140**, A769 (1965).
[12]A. V. Phelps, J. Phys. Chem. Ref. Data **19**, 653 (1990).
[13]T. A. Thorson, R. D. Durst, R. J. Fonck, and L. P. Wainwright, Phys. Plasmas **4**, 4 (1997).
[14]T. A. Thorson, R. D. Durst, R. J. Fonck, and A. C. Sontag, Nucl. Fusion **38**, 495 (1998).